Genetic risk for Parkinson's disease correlates with alterations in neuronal manganese sensitivity between two human subjects.

By: Asad A. Aboud, Andrew M. Tidball, Kevin K. Kumar, M. Diana Neely, Kevin C. Ess, Keith M. Erikson, and Aaron B. Bowman

Aboud AA, Tidball AM, Kumar KK, Neely MD, Ess KC, Erikson KM, Bowman AB. (2012) Genetic risk for Parkinson's disease correlates with alterations in neuronal manganese sensitivity between two human subjects. *Neurotoxicology*. 33(6):1443-1449.

Abstract:

Manganese (Mn) is an environmental risk factor for Parkinson's disease (PD). Recessive inheritance of PARK2 mutations is strongly associated with early onset PD (EOPD). It is widely assumed that the influence of PD environmental risk factors may be enhanced by the presence of PD genetic risk factors in the genetic background of individuals. However, such interactions may be difficult to predict owing to the complexities of genetic and environmental interactions. Here we examine the potential of human induced pluripotent stem (iPS) cell-derived early neural progenitor cells (NPCs) to model differences in Mn neurotoxicity between a control subject (CA) with no known PD genetic risk factors and a subject (SM) with biallelic loss-of-function mutations in PARK2 and family history of PD but no evidence of PD by neurological exam. Human iPS cells were generated from primary dermal fibroblasts of both subjects. We assessed several outcome measures associated with Mn toxicity and PD. No difference in sensitivity to Mn cytotoxicity or mitochondrial fragmentation was observed between SM and CA NPCs. However, we found that Mn exposure was associated with significantly higher reactive oxygen species (ROS) generation in SM compared to CA NPCs despite significantly less intracellular Mn accumulation. Thus, this report offers the first example of human subject-specific differences in PD-relevant environmental health related phenotypes that are consistent with pathogenic interactions between known genetic and environmental risk factors for PD.

Keywords: Parkinson's disease | manganese | human induced pluripotent stem cells | gene–environment interactions | neurotoxicology

Article:

1. Introduction

Parkinson's disease (PD), the second most common neurodegenerative disorder, is clinically characterized by bradykinesia, resting tremor, rigidity, and loss of postural reflexes. PD etiology is largely unknown but there is strong evidence to implicate environmental risk factors, especially exposure to heavy metals and pesticides, in its pathogenesis (Elbaz and Moisan, 2010, Schapira, 2011 and Tanner et al., 2011). Exposure to Mn is an important environmental risk factor for PD (Aschner and Erikson, 2009, Bowman et al., 2011 and Guilarte, 2010). Exposure to very high concentrations of Mn causes manganism, a syndrome that shares many features with PD (Guilarte, 2010, Lucchini et al., 2009, Olanow, 2004 and Racette et al., 2011). High levels of Mn in the ambient air has been associated with earlier age of onset for PD, indicating that Mn may accelerate the process of age-related neuronal loss (Finkelstein and Jerrett, 2007). Manganism most frequently occurs from occupational Mn exposure such as may occur in mining, welding metals, and dry battery manufacturing (Keen et al., 2000). However, a more insidious course due to a cumulative exposure to small doses over a long period of time is also possible (Lucchini et al., 2009). A prospective study assessing the long term neurotoxic effects of Mn exposure in bridge construction workers has concluded that while cognitive decline improved in previous workers after 3.5 years follow up, motor and mood disturbances precipitated by Mn exposure were persistent despite decreasing blood Mn levels (Bowler et al., 2011). Moreover, it has been shown that Mn exposure causes up regulation of α-synuclein (SCNA) and down regulation of Tyrosine hydroxylase (TH) and Parkin (PARK2) in dopaminergic neurons, resulting in increased oxidative stress and eventual cell death (Wang et al., 2009).

The mechanisms by which Mn exerts its neurotoxic effects are not well understood. Some of the proposed mechanisms include disruption of mitochondrial metabolism (Zhang et al., 2008) and oxidative stress (Zhang et al., 2004). The influence of Mn exposure on individuals is determined by a combination of variables including age and nutritional status (Aschner and Erikson, 2009). Nonetheless, the neurotoxic effects of Mn tend to vary greatly between individuals (Roth, 2006). This variation is most likely due to genetic variability that renders an individual more or less sensitive to the toxic effects of Mn which eventually manifests in variable clinical course (Roth, 2006). For example, the cytotoxic effect of Mn is dependent on its intracellular levels (Yin et al., 2010) and genetic variations like polymorphisms and copy number variations involving key components of Mn transport such as DMT1 (He et al., 2011) and the iron/Mn exporter ferroportin (Yin et al., 2010) can alter Mn sensitivity. Thus genetic variation between individuals, which cannot be readily quantified or studied, using established model systems, complicates assessment of personalized risk to Mn exposure.

Genetic susceptibility plays a significant role in the pathogenesis of PD. One study indicated a concordance rate for nigrostriatal dysfunction at 45% in monozygotic twins where one twin has a PD diagnosis (Burn et al., 1992). The concordance rate of subclinical dopaminergic dysfunction might be even higher (75%) in monozygotic twins as assessed by positron emission tomography

(Piccini et al., 1999). Of importance, for a subset of PD patients the disease can be directly linked to inheritance of a monogenic risk factor (Gasser, 2009 and Lesage and Brice, 2009). Loss of function mutations in PARK2, which encodes the E3 ubiquitin ligase Parkin, is the most common cause of autosomal recessive PD (Kitada et al., 1998). Loss of Parkin is associated with mitochondrial dysfunction and cytotoxicity suggesting a neuroprotective role involving maintenance of mitochondrial integrity (Narendra et al., 2008 and Narendra et al., 2009). Further highlighting its role in neuroprotection, PARK2 over expression was shown to rescue dopaminergic neurons from cell death caused by Mn toxicity (Higashi et al., 2004).

Manganism and familial cases of PD represent the opposite ends of the environmental versus genetic etiology of parkinsonian pathologies. However, complex interactions between environmental and genetic risk factors likely underlie the majority of idiopathic PD cases. These genetic risk factors may include susceptibility genes that increase PD risk but may not directly cause disease (Vance et al., 2010). Furthermore, even in the presence of a strong PD genetic risk factor, like biallelic inheritance of PARK2 loss-of-function mutations, there is a wide variation in age-of-onset with documented cases of asymptomatic individuals many decades older than family members with inheritance of the same monoallelic genetic risk factor (Marder et al., 2010 and von Coelln et al., 2004). A particularly relevant example is a 56-year old patient with no evidence of Parkinsonism despite inheritance of compound heterozygous mutations in PARK2 (Deng et al., 2006). Remarkably, four siblings of this patient who inherited the identical mutations in maternal and paternal alleles were diagnosed with EOPD (age of onset ranging from 30 to 38 years old). Thus, even under conditions of the relatively minimal genetic variation of a single family, other genetic and/or environmental factors play a critical role in the pathogenesis of PD.

Here we tested the hypothesis that two human subjects with distinct genetic risk profiles for PD would display differences in the vulnerability of NPCs to Mn exposure, a major PD environmental risk factor. The two subjects are identified here as “CA”, a male healthy control with no family history of PD; and “SM”, a male subject with compound heterozygous loss-of-function mutations in PARK2 and a family history of EOPD in his full sibling with the same PARK2 genotype. Despite the family history and the genetic background, SM, age 43, has no evidence of PD on neurological exam. The approach we took to test our hypothesis utilized iPS cell technology to make subject-specific NPCs via a dual-SMAD inhibition differentiation (Chambers et al., 2009, Hao et al., 2010, Neely et al., 2012 and Takahashi et al., 2007). Human iPS derived cells retain the unique genetic characteristics of each research subject, thus offering the possibility of modeling personalized environmental risk to Mn toxicity (Kumar et al., 2012). We assessed Mn neurotoxicity in SM and CA derived NPCs focusing on the PD-relevant outcome measures of cell death, mitochondrial fragmentation, oxidative stress and cellular Mn

accumulation. We report patient-specific differences in Mn accumulation and reactive oxygen species generation. This report provides proof of principle for detecting gene–environment interactions between human subjects and a neurotoxicant using an iPS cell-based model system.

2. Materials and methods

2.1. iPS cells generation, validation, and maintenance

We derived the lines used in our work from two subjects through either viral- or episomal-mediated reprogramming as described previously (Okita et al., 2011 and Takahashi et al., 2007). Punch skin biopsies were used to obtain primary epidermal fibroblasts from subjects CA and SM under Vanderbilt IRB#080369 (KE). The first two letters of every line designates the de-identified human subject, while the numeral following designates each independent iPS line. Lines generated through viral transduction include CA4, CA6, SM3, SM4, SM5, and lines generated through the non-integrating episomal method include CA11, SM14. The PARK2 mutation in SM fibroblasts, first identified by clinical genetic tests, was confirmed through sequencing of cDNA to be a 40 bp deletion in exon 3 of one allele and a complete deletion of exons 5 and 6 on the other allele (manuscript submitted). All lines were validated for the expression of pluripotency markers by immunocytochemistry and quantitative reverse-transcriptase (QRT-PCR). Chromosomal euploidy was confirmed by karyotyping for all lines by Genetic Associates Inc. (Nashville, TN). Additional information on the generation, validation, and maintenance of the iPS lines is described in detail elsewhere (Neely et al., 2012).

2.2. Neural induction and splitting of NPCs

NPCs were generated by adapting a dual-SMAD inhibition protocol developed by Lorenz Studer (Sloan-Kettering Institute, NY) and colleagues (Chambers et al., 2009) substituting the Bone Morphogenetic Protein (BMP) inhibitor DMH1 for Noggin (Neely et al., 2012). Our method of NPCs differentiation is described in detail elsewhere (Neely et al., 2012). These early neuronal precursors express PAX6, a marker of human neural ectoderm, as well as FOXG1, OTX2 and SOX1 and are thought to be the first stage in neuronal lineage commitment (Zhang et al., 2010). In brief, neural induction begins on what is designated as day 1 when the neuralization medium (Knockout DMEM/F12, 15% KSR, Glutamax (all from Invitrogen), penicillin/streptomycin (Mediatech), nonessential amino acids, and 55 μM β-mercaptoethanol (both from Sigma)) containing 10 μM SB431542 (Tocris) and 0.5 μM DMH1 (gift from Dr. Charles Hong, Vanderbilt University) is added to the iPS cells approximately four days after their initial plating on Matrigel-coated wells (BD Biosciences, San Jose, CA; Fig. 1). Neuralization continues for 7 days, which coincides with high expression of PAX6, the main NPC marker used in this study (Neely et al., 2012). Most of the experiments include splitting of NPCs on day 6 of neuralization

to either control for the cell count (in cell survival and ROS experiments) or to enable clear visualization of mitochondrial morphology in mitochondrial fragmentation analysis studies.

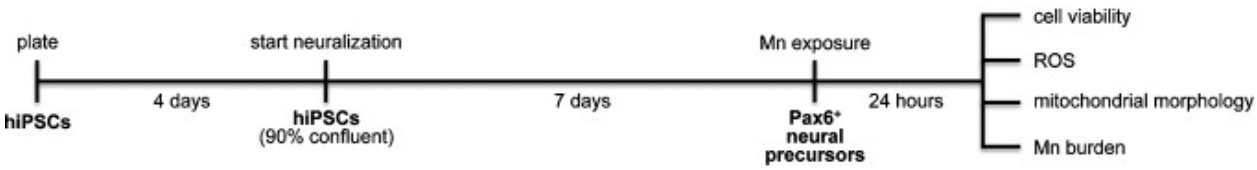

Fig. 1. Experimental design. iPS cells were plated for each experiment on Matrigel-covered 12 well or 96 well plates at a density of 6 × 104 cell/ml. On the fourth day after plating they reach a confluency of approximately 90% and that is when neuralization starts (day 1) with the dual-SMAD inhibition protocol. On day 7 of neuralization 80–90% of the cell population in culture are NPCs (PAX6+). We exposed the cells in all of our experiments on day 7 for 24 h followed by assessment of Mn-related outcome measures.

NPCs were split on day 6 of neuralization for these experiments: MTT survival assay, measurement of ROS, and assessment of mitochondrial fragmentation. Briefly, cells were washed once with DMEM-F12 (Invitrogen) and treated with 500 μl Accutase (Innovative Cell Technologies, San Diego, CA) per one well of a 12 well plate for 8–10 min at 37 °C. Another 500 μl of neuralization medium was added to each well and the cells were thoroughly pipetted and transferred to a 15 ml conical tube and centrifuged (200 × g for 5 min). Cells were resuspended in 1 ml neuralization medium that contains 10 μM Rho-Kinase (ROCK) inhibitor, Y-27632 (Tocris), 10 μM SB431542 and 0.5 μM DMH1. NPCs were plated on Matrigel pre-coated plates in this same medium in an assay-dependent cell density specified below.

2.3. Cell viability assay

Cell viability was assessed by splitting NPCs on day 6 of neural induction onto Matrigel-covered 96 well plates at a density of 2 × 105 cell/ml. 500 or 1000 μM MnCl2 was added to the neuralization medium on day 7 of neuralization. After 24 h of exposure the neuralization medium was removed and the NPCs were washed once with PBS. Incubation with MTT (3-(4,5-dimethylthiazol-2-yl)-2,5-diphenyltetrazolium bromide) (Research Organics) dye in neuralization medium followed for two and a half hours (Williams et al., 2010). The medium was subsequently removed, and cells were solubilized using 10% Sorenson's buffer in DMSO. Absorbance was read at 570 nM using a DTX 880 Multiplate Reader (Beckman Coulter). Absorbance was normalized to the vehicle-only exposed controls of each genotype for each independent experiment. Data were plotted using Prism5 (GraphPad) and analysis was performed using two-way ANOVA. The alpha level was set at $p < 0.05$.

2.4. Quantification of Mn induced ROS production

NPCs were split on day 6 of neuralization at a cell density of 2 × 105 cell/ml. On day 7 of neuralization, cells were washed twice with 100 μl KR-HEPES buffer. They were then incubated with 2 μM of the dichlorodihydrofluorescein-based dye CM-H2DCFDA (Invitrogen) in KR-HEPES in the dark at 37 °C for 30 min. Cells were washed 3 times with 100 μl of KR-HEPES and the experimental conditions were added in KR-HEPES. Fluorescent measurements were taken using a Beckman Coulter DTX 880 microplate reader at 37 °C. The excitation wavelength was 485 nm (filter bandwidth ± 20 nm) and emission 535 nm (filter bandwidth ± 25 nm). Absorbance was normalized to the vehicle-only exposed controls of each genotype for each independent experiment. Two-way ANOVA was used for statistical analysis of log-transformed data; a Bonferroni test was used for post hoc analysis (Prism software).

2.5. Mitochondrial fragmentation analysis

NPCs were split on day 6 of neuralization and were re-plated on Matrigel coated 8 well glass slides (Thermo Scientific) with a density of 1 × 105 cells/ml. On day 7 of neuralization NPCs were exposed to either vehicle or 500 μM Mn. After 24 h of exposure NPCs were incubated with 100 nM MitoTracker Red dye (Invitrogen) in neuralization medium for 45 min at 37 °C. The dye-containing medium was subsequently taken off and cells were incubated in dye-free neuralization medium for 10 min. Cells were washed once with PBS and fixed with 4% paraformaldehyde for 10–15 min at room temperature. Alternatively, the mitochondria-specific viral transduction system (CellLight Mitochondria-GFP, Backmam 2.0; Invitrogen) was used to label mitochondria. In this method, the reagent was added to NPCs on day 6 of neutralization during re-plating at a multiplicity of infection (MOI) of 20. NPCs were exposed after 24 h to either vehicle or Mn for another 24 h then fixed as specified above. Subsequently, NPCs were stained with PAX6 antibody (Neely et al., 2012), followed by nuclear counter staining using 2 μM TO-PRO-3 dye (Invitrogen) for 10 min. The slides were cover-slipped with No. 1 cover slips using ProLong Gold mounting medium (Invitrogen). Confocal microscopy was used to assess mitochondrial morphology using a 63× objective lens. Analysis was done with blinding to the genotypes and exposure conditions. 50 PAX6+ cells per each condition were assessed for mitochondrial fragmentation (Lutz et al., 2009 and Sterky et al., 2011) in each experiment with cells chosen randomly from each of the four well quadrants. Apoptotic and mitotic cells were identified by morphology (shrunken cells with condensed nuclei and cells with fused nuclei, respectively) and excluded from the analysis. We developed a severity scale of four scores from 1 to 4 to visually assess mitochondrial fragmentation. A score of one indicates that the cell has minimal mitochondrial fragmentation (<25%) with intact network formation, while a score of 4 indicates severe mitochondrial fragmentation (>75%) with complete loss of mitochondrial tubular structure. Scores 2 and 3 indicate moderate mitochondrial fragmentation with some intact network structure, and moderate to severe fragmentation with only sparse mitochondrial tubular

structure, respectively. The average mitochondrial fragmentation score of all assessed cells in an experimental condition reflects the overall severity of mitochondrial fragmentation. Statistical analysis was performed using two-way ANOVA on the log transformed average scores of all cells in each experiment using SPSS software, with a paired two-tailed t-test for post hoc analysis.

2.6. Graphite furnace atomic absorption spectrometry (GFAAS)

SM and CA NPCs differentiated on 12 well plates were treated with 500 μM $MnCl_2$ on day 7 of neuralization for 24 h. Cells were washed once with PBS (1 ml/well). 250 μl of PBS was then added to each well. Cells were then scraped mechanically and flash frozen in liquid nitrogen then stored in −80 °C for two weeks. Total Mn level was analyzed in 3 independent vehicle-treated samples and 4 independent Mn-treated samples by GFAAS using a modified version of our published methods (Williams et al., 2010 and Yin et al., 2010). Bovine liver (NBS Standard Reference Material, USDC, Washington, DC) (10 μg Mn/g) was digested in ultrapure nitric acid and used as an internal standard for analysis (final concentration 10 μg Mn/L) as published previously (Anderson et al., 2009). Findings are reported as total Mn level (μg) normalized to total protein (mg). Data were analyzed by two-way ANOVA (Prism5 software, GraphPad) and the alpha level was set at $p < 0.05$.

3. Results

3.1. CA and SM NPCs exhibit identical sensitivity to acute Mn-induced cell death

To test the hypothesis that NPCs from subjects CA and SM differ in their sensitivity to Mn cytotoxicity (i.e. cell death) we examined cell survival of day 7 NPCs following 24 h exposure to Mn. In a parallel study we determined the EC50 value for cell survival (by MTT assay) following 24-h Mn exposure using a concentration response curves (manuscript submitted). This analysis revealed an EC50 value of 1200 μM $MnCl_2$ for cell death following Mn exposure. Furthermore, no significant differences were observed between CA and SM survival curves (data not shown). To increase statistical power for detection of subtle differences in sensitivity to Mn exposure we assessed cell viability of NPCs at 500 μM and 1000 μM $MnCl_2$ using two independent control lines (CA6 and CA11) and three independent SM lines (SM3, SM5 and SM14) (Fig. 2). We did not detect a significant difference in Mn cytotoxicity between SM and CA NPCs. Thus SM and CA NPCs display statistically identical sensitivities to acute Mn-induced cell death.

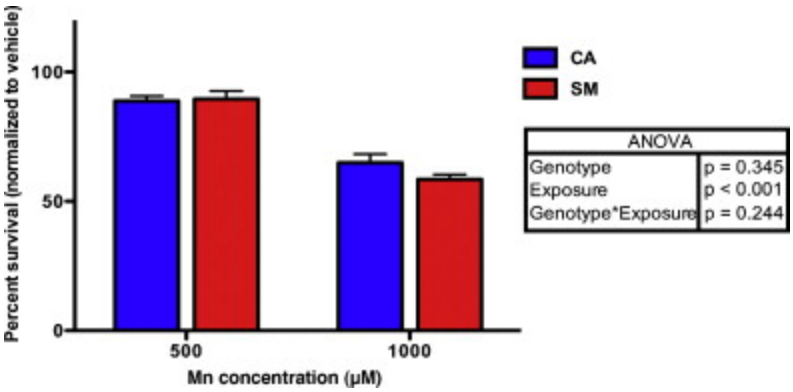

Fig. 2. Mn cytotoxicity in NPCs. CA and SM NPCs were treated with Mn and cell viability was assessed using MTT assay. Two-way ANOVA revealed significant exposure effect ($p < 0.001$) without a significant genotype effect ($p = 0.345$). CA lines used in this experiment include CA6 ($n = 2$) and CA11 ($n = 2$), and SM lines include SM3 ($n = 1$), SM5 ($n = 1$), and SM14 ($n = 1$). Data are collected from 3 independent replicates. Error bars represent SEM.

3.2. CA and SM NPCs generate elevated Mn-dependent reactive oxygen species (ROS)

Although no differences in sensitivity to Mn cytotoxicity were found, we tested the hypothesis that SM NPCs may be more prone to ROS generation after Mn exposure. Mn neurotoxicity has been linked to the enhanced generation of ROS (Gunter et al., 2004 and Tamm et al., 2008). Moreover, Parkin (protein product of the PARK2 gene) has been implicated in maintenance of mitochondrial turnover and loss of this function might predispose cells to generate higher ROS (Koh and Chung, 2010). We tested the levels of ROS in CA and SM NPCs by using the ROS-sensitive dye 2′,7′-dichlorofluorescein (DCF) following Mn exposure. We found that SM NPCs generated increased DCF detected ROS relative to CA NPCs after 30 min $MnCl_2$ exposure (Fig. 3). Two-way ANOVA of both low and high Mn exposure levels identified a significant genotype effect ($p = 0.001$). Bonferroni post hoc analysis showed a significant difference between SM and CA at both 500 μM ($p < 0.05$) and 1000 μM ($p < 0.01$) Mn exposures.

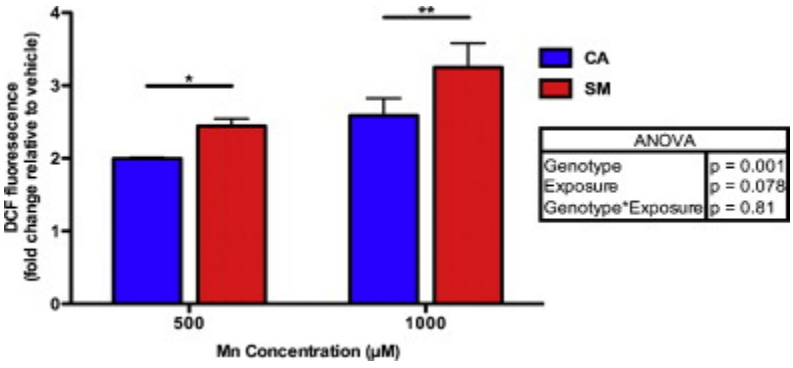

Fig. 3. ROS generation in NPCs. NPCs are treated with two concentrations of manganese and the level of ROS generation was assessed using DCF dye. Two-way ANOVA on the log-transformed values returned genotype difference ($p = 0.001$) but no genotype × exposure

interaction. CA lines used in these experiments include CA6 (n = 2–3) and CA11 (n = 2–3); and SM lines include SM3 (n = 2–3) and SM14 (n = 2–3). Data are collected from four independent 500 μM and six independent 1000 μM MnCl2 experiments. Error bars represent SEM.

3.3. Increase in Mn-dependent mitochondrial fragmentation is similar between CA and SM

Loss of PARK2 function has been associated with increased mitochondrial fragmentation (Greene et al., 2003 and Lutz et al., 2009). We hypothesized that Mn exposure, which is known to cause mitochondrial dysfunction (Brown and Taylor, 1999 and Malecki, 2001), would cause more mitochondrial fragmentation in SM NPCs than CA. We found that Mn exposure was associated with increased mitochondrial fragmentation, as assessed using MitoTracker Red dye, in both CA and SM NPCs (Fig. 4). Two-way ANOVA of the average mitochondrial fragmentation score revealed a highly significant Mn exposure effect (p = 0.008) with no significant differences by genotype (p = 0.44) nor the two-way interaction term (p = 0.269).

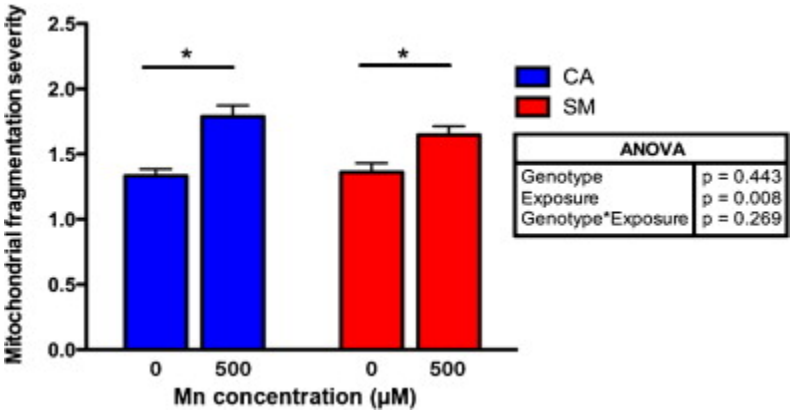

Fig. 4. Quantification of mitochondrial fragmentation in NPCs using MitoTracker Red. CA and SM NPCs are treated with 500 μM MnCl2 for 24 h followed by mitochondrial staining using MitoTracker Red dye (100 nM). 50 PAX6+ cells were counted for each condition and scored from 1 to 4 increasing with severity of mitochondrial fragmentation. The average score of cells assessed for three independent experiments after exposure to 0 or 500 μM Mn. Two-way ANOVA on the log-transformed data returned high significance for the effect of Mn exposure, but no genotype or genotype × exposure interaction effects. Paired two-tailed t-test was used for post hoc analysis of the three independent paired experiments: CA6 with SM4 (n = 1), and CA6 with SM5 (n = 2). Error bars represent SEM.

In an independent set of experiments, we used the CellLight Mitochondria-GFP transduction system as an alternative approach to assess mitochondrial morphology. This mitochondria labeling system utilizes Baculovirus particles to deliver a GFP fusion protein with the leader sequence of the E1 alpha pyruvate dehydrogenase that is specific to mitochondria. Unlike MitoTracker Red dye, CellLight reagent does not rely on membrane potential for mitochondrial localization. This property makes CellLight a control for the possible influence of decreased membrane potential due to Mn exposure on our assessment of mitochondrial morphology by

MitoTracker Red. We found that, compared to vehicle-exposed NPCs, Mn exposure was associated with increased mitochondrial fragmentation and disruption of the mitochondrial tubular structure (Fig. 5). Two-way ANOVA of mean mitochondrial fragmentation scores performed on this independent set of experiments also revealed a significant Mn exposure effect ($p = 0.0019$), with no significant differences by genotype ($p = 0.556$) or the two-way interaction term ($p = 0.956$). Thus both methods of mitochondrial labeling revealed comparable influence of Mn on mitochondrial fragmentation with no significant effect of genotype.

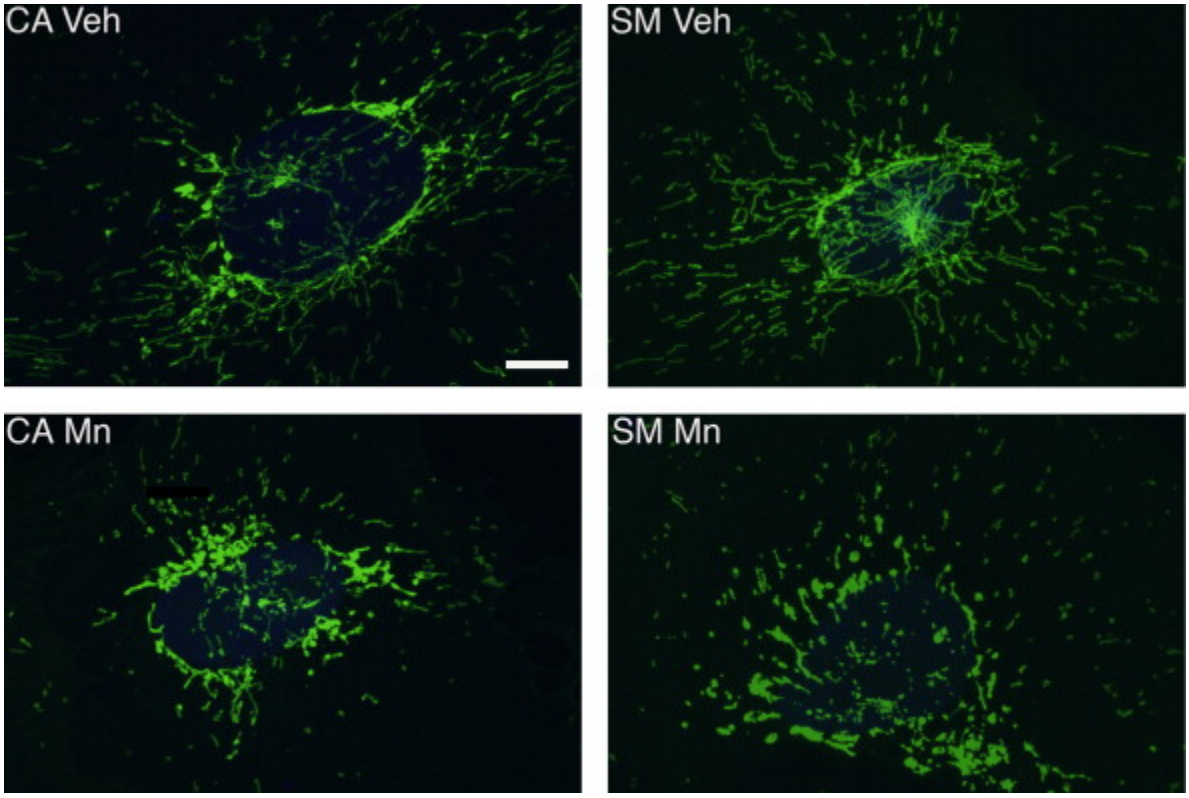

Fig. 5. Quantification of mitochondrial fragmentation in NPCs using CellLight Mitochondria-GFP. Representative images are shown for CA and SM vehicle- and Mn-treated NPCs after staining with CellLight Mitochondria-GFP and TO-PRO-3 nuclear counterstain. PAX6+ NPCs were analyzed for mitochondrial fragmentation as described in Section 2.5. (CA6: SM3 n = 2, CA11:SM14 n = 1). Scale bar = 10 μm.

3.4. Decreased net Mn uptake in SM NPCs versus CA

The data above indicated enhanced ROS generation in SM NPCs compared to CA after Mn exposure despite similar effects on cell survival and mitochondrial morphology. Thus we tested the hypothesis that SM NPCs may accumulate increased levels of intracellular Mn following exposure. This is especially relevant given the evidence for Parkin involvement in manganese transport through degradation of DMT1 (Roth et al., 2010). Remarkably, we found that SM NPCs accumulated about 35% less intracellular Mn than CA NPCs after Mn exposure (Fig. 6).

Two-way ANOVA revealed a highly significant main effect of genotype ($p = 0.009$), exposure ($p < 0.001$), and genotype × exposure interaction ($p = 0.014$).

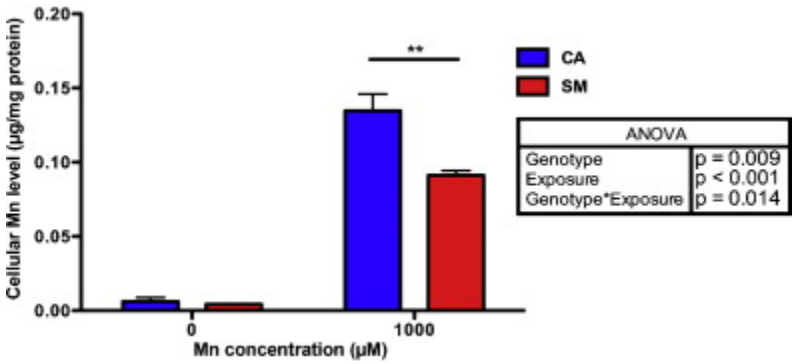

Fig. 6. Measurement of total Mn accumulation in SM and CA NPCs using (GFAAS). Intracellular Mn accumulation was assessed in CA and SM NPCs after exposure to vehicle and 500 µM Mn. Outputs were normalized to the protein concentration of each sample. Two-way ANOVA revealed significant genotype difference in total Mn level after Mn exposure ($p = 009$). CA6 and SM5 lines were used in these experiments. Data are collected from 3 independent vehicle exposed samples and 4 independent Mn treated samples. Error bars represent SEM.

4. Discussion

We report here a proof-of-principle study to evaluate the potential of patient stem cell derived neuronal models to predict the contribution of individual genetic variability to Mn neurotoxicity by examining early neural progenitors of two human subjects with disparate genetic risk factors for PD. We present a case of a subject (SM) having a family history (an affected sibling) as well as inheritance of a known PD genetic risk factor (compound heterozygous mutations in PARK2) versus another subject (CA) with no know PD genetic risk factors or family history of PD. We focused on outcome measures functionally linked to PARK2 gene function and Mn toxicity such as regulation of mitochondrial biogenesis and turnover (Koh and Chung, 2010, Lutz et al., 2009 and Yin et al., 2008) and Mn transport (Roth et al., 2010). We found that exposure of human NPCs to Mn resulted in cell death, increased ROS generation, and mitochondrial fragmentation. ROS generation was significantly higher in SM-derived NPCs compared to CA-derived NPCs. This suggests enhanced sensitivity of SM NPCs to Mn exposure, especially considering the significantly lower Mn accumulation in SM NPCs compared to CA after Mn exposure. Thus, the near equivalent cytotoxicity and mitochondrial fragmentation in CA and SM NPCs occurs in the face of significantly less intracellular Mn in the SM-derived cells. We propose that the enhanced susceptibility of SM NPCs to the deleterious effects of Mn is due to differences in susceptibility to intracellular Mn despite equivalent cellular accumulation of the metal. This could be due to failure of one or more cellular mechanisms that are normally involved in maintaining normal homeostasis during stress, such as oxidative stress response mechanisms and mitochondrial biogenesis rates. Furthermore, the decreased net uptake of Mn in the SM NPCs suggests the

possibility of the activation of compensatory mechanisms to limit Mn toxicity in the face of heightened sensitivity. Together, our data strongly indicate that NPCs from a human subject with strong PD genetic risk factors have elevated sensitivity to Mn neurotoxicity compared to a subject without these risk factors.

Mn concentrations used in this study are slightly higher (about 2- to 3-fold) than typically seen in vivo following pathophysiological Mn exposure. Normally, brain Mn levels average around 1–2 μg/g (18–36 μM) with the highest level being in the globus pallidus in human and hypothalamus in rats (Bowman et al., 2011 and Prohaska, 1987). Studies in rodents indicate that these concentration increase by a magnitude of approximately 2- to 10-fold after acute Mn exposure (Madison et al., 2012). Concentrations as high as 500 μM fail to produce significant cytotoxicity over the exposure durations (up to 48 h) in NPCs. This is consistent with in vivo data wherein acute exposure to Mn, during which brain Mn levels likely do not exceed ~400 μM, is not associated with substantial neurodegeneration (Madison et al., 2012). Moreover, other groups have reported similar sensitivities of culture human cells to Mn (Roth et al., 2000 and Roth et al., 2012). One reasonable explanation for the apparent resistance of cells to high concentrations of Mn in tissue culture media could be the binding of Mn to serum proteins and other constituents of media that decrease the availability of free Mn.

Although a previous study showed that Parkin promotes degradation of the 1B isoform of DMT1 and lowers Mn levels consequently (Roth et al., 2010), the influence of long-term loss of human PARK2 expression in the context of neural lineages has not been examined. One possible hypothesis to explain the differential accumulation of Mn is a potential discrepancy is cellular compensation of SM cells in response to a heighten sensitivity to Mn toxicity. One mechanism by which this may occur would be to increase efflux of Mn via metal exporters such as ferroportin (Yin et al., 2010). Another intriguing possibility could be human genetic variation outside of the PARK2 mutation that influences cellular Mn status.

The finding of mitochondrial dysfunction in human NPCs after Mn exposure is not surprising given the previously reported observation of mitochondrial toxicity in other model systems (Malecki, 2001 and Zhang et al., 2008). The assessment of Mn-related ROS generation and mitochondrial dysfunction in human-derived neurons is an important advancement, however, as it has the potential to answer important questions about the subject-specific susceptibility to Mn and other compounds.

In conclusion, we show here a strong proof-of-principle support for the modeling of subject-specific human Mn neurotoxicity using iPS model system. We have demonstrated that, in this example, a human subject with a family history of PD and inheritance of a strong genetic risk factor for PD exhibited elevated susceptibility to disease relevant Mn toxicity than iPS-derived NPCs from a control subject. Our findings appear to suggest a potentially protective cellular response to decrease Mn accumulation upon exposure and thereby attenuate Mn-dependent phenotypes. Further studies should be carried out to understand whether the decreased Mn accumulation is functionally linked to the PARK2 mutation or other genetic factors. Future experiments might also reveal a different sensitivity profile of neurons as they are differentiated further down the nigral dopaminergic lineage toward the vulnerable neuronal population in PD.

Conflict of interest

None.

Acknowledgements

We would like to thank Dr. Peter Hedera (Vanderbilt University, TN) for identifying patient SM. We are grateful to Dr. Charles Hong (Vanderbilt University, TN) for generously providing the BMP inhibitor DMH1 for these studies. We would like also to thank Bingying Han, Bryan Cawthon, and Chris Jetter, for technical assistance. We thank Dr. Reed Chamberlin and Dr. V.G. Dev of Genetics Associates, Inc. (Nashville, TN) for karyotyping analyses. This work has been supported by the following grants: NIH/NIEHSES016931 (ABB) and ES016931-02S1 (ABB), NICHD P30HD15052 to Vanderbilt University, Vanderbilt University, PK Hope is Alive! (ABB), subaward RR166-737/4787736 under NIH/NIGMS 5PO1GM08535403 (ABB and KE), Vanderbilt Center for Molecular Toxicology Pilot Project under NIH/NIEHS 5P30ES000267 (ABB, DN), Peterson Foundation for Parkinsons (ABB), NIH/NINDSNS078289 (KE), Doris Duke Charitable Foundation (KE), VICTR Grant (ABB, KE), additional support by the Vanderbilt Kennedy Center, NIH/NICHDP30HD15052 and the Vanderbilt Medical Scientist Training Program NIH/NIGMS T32GM07347 (KK). The content is solely the responsibility of the authors and does not necessarily represent the official views of the NIH/NIEHS. Finally we would like to thank the Department of Neurology and the Vanderbilt Kennedy Center for their support.

References

J.G. Anderson, S.C. Fordahl, P.T. Cooney, T.L. Weaver, C.L. Colyer, K.M. Erikson. Extracellular norepinephrine, norepinephrine receptor and transporter protein and mRNA levels

are differentially altered in the developing rat brain due to dietary iron deficiency and manganese exposure. Brain Res, 1281 (2009), pp. 1–14

M. Aschner, K.M. Erikson, E. Herrero Hernandez, R. Tjalkens. Manganese and its role in Parkinson's disease: from transport to neuropathology. Neuromol Med, 11 (2009), pp. 252–266

R.M. Bowler, V. Gocheva, M. Harris, L. Ngo, N. Abdelouahab, J. Wilkinson et al. Prospective study on neurotoxic effects in manganese-exposed bridge construction welders. Neurotoxicology, 32 (2011), pp. 596–605

A.B. Bowman, G.F. Kwakye, E.H. Hernandez, M. Aschner. Role of manganese in neurodegenerative diseases. J Trace Elem Med Biol, 25 (2011), pp. 191–203

S. Brown, N.L. Taylor. Could mitochondrial dysfunction play a role in manganese toxicity. Environ Toxicol Pharmacol, 7 (1999), pp. 49–57

D.J. Burn, M.H. Mark, E.D. Playford, D.M. Maraganore, T.R. Zimmerman Jr., R.C. Duvoisin et al. Parkinson's disease in twins studied with 18F-dopa and positron emission tomography. Neurology, 42 (1992), pp. 1894–1900

S.M. Chambers, C.A. Fasano, E.P. Papapetrou, M. Tomishima, M. Sadelain, L. Studer. Highly efficient neural conversion of human ES and iPS cells by dual inhibition of SMAD signaling. Nat Biotechnol (2009), pp. 275–280

H. Deng, W.D. Le, C.B. Hunter, W.G. Ondo, Y. Guo, W.J. Xie et al. Heterogeneous phenotype in a family with compound heterozygous parkin gene mutations. Arch Neurol, 63 (2006), pp. 273–277

A. Elbaz, F. Moisan. Parkinson's disease: Is there a strong environmental contribution? Rev Neurol (Paris), 166 (2010), pp. 757–763

M.M. Finkelstein, M. Jerrett. A study of the relationships between Parkinson's disease and markers of traffic-derived and environmental manganese air pollution in two Canadian cities. Environ Res, 104 (2007), pp. 420–432

T. Gasser. Mendelian forms of Parkinson's disease. Biochim Biophys Acta, 1792 (2009), pp. 587–596

J.C. Greene, A.J. Whitworth, I. Kuo, L.A. Andrews, M.B. Feany, L.J. Pallanck. Mitochondrial pathology and apoptotic muscle degeneration in Drosophila parkin mutants. Proc Natl Acad Sci USA, 100 (2003), pp. 4078–4083

T.R. Guilarte. Manganese and Parkinson's disease: a critical review and new findings. Environ Health Perspect, 118 (2010), pp. 1071–1080

T.E. Gunter, L.M. Miller, C.E. Gavin, R. Eliseev, J. Salter, L. Buntinas et al. Determination of the oxidation states of manganese in brain, liver, and heart mitochondria. J Neurochem, 88 (2004), pp. 266–280

J. Hao, J.N. Ho, J.A. Lewis, K.A. Karim, R.N. Daniels, P.R. Gentry et al. In vivo structure-activity relationship study of dorsomorphin analogues identifies selective VEGF and BMP inhibitors. ACS Chem Biol, 5 (2010), pp. 245–253

Q. He, T. Du, X. Yu, A. Xie, N. Song, Q. Kang et al. DMT1 polymorphism and risk of Parkinson's disease. Neurosci Lett, 501 (2011), pp. 128–131

Y. Higashi, M. Asanuma, I. Miyazaki, N. Hattori, Y. Mizuno, N. Ogawa. Parkin attenuates manganese-induced dopaminergic cell death. J Neurochem, 89 (2004), pp. 1490–1497

C.L. Keen, J.L. Ensunsa, M.S. Clegg. Manganese metabolism in animals and humans including the toxicity of manganese. Met Ions Biol Syst, 37 (2000), pp. 89–121

T. Kitada, S. Asakawa, N. Hattori, H. Matsumine, Y. Yamamura, S. Minoshima et al. Mutations in the parkin gene cause autosomal recessive juvenile parkinsonism. Nature, 392 (1998), pp. 605–608

H. Koh, J. Chung. PINK1 and Parkin to control mitochondria remodeling. Anat Cell Biol, 43 (2010), pp. 179–184

K.K. Kumar, A.A. Aboud, A.B. Bowman. The potential of induced pluripotent stem cells as a translational model for neurotoxicological risk. Neurotoxicology, 33 (3) (2012), pp. 518–529

S. Lesage, A. Brice. Parkinson's disease: from monogenic forms to genetic susceptibility factors. Hum Mol Genet, 18 (2009), pp. R48–R59

.G. Lucchini, C.J. Martin, B.C. Doney. From manganism to manganese-induced parkinsonism: a conceptual model based on the evolution of exposure. Neuromol Med, 11 (2009), pp. 311–321

A.K. Lutz, N. Exner, M.E. Fett, J.S. Schlehe, K. Kloos, K. Lammermann et al. Loss of parkin or PINK1 function increases Drp1-dependent mitochondrial fragmentation. J Biol Chem, 284 (2009), pp. 22938–22951

J.L. Madison, M. Wegrzynowicz, M. Aschner, A.B. Bowman. Disease-toxicant interactions in manganese exposed Huntington disease mice: early changes in striatal neuron morphology and dopamine metabolism. PLoS One, 7 (2012), p. e31024

E.A. Malecki. Manganese toxicity is associated with mitochondrial dysfunction and DNA fragmentation in rat primary striatal neurons. Brain Res Bull, 55 (2001), pp. 225–228

K.S. Marder, M.X. Tang, H. Mejia-Santana, L. Rosado, E.D. Louis, C.L. Comella et al. Predictors of parkin mutations in early-onset Parkinson disease: the consortium on risk for early-onset Parkinson disease study. Arch Neurol, 67 (2010), pp. 731–738

D. Narendra, A. Tanaka, D.F. Suen, R.J. Youle. Parkin is recruited selectively to impaired mitochondria and promotes their autophagy. J Cell Biol, 183 (2008), pp. 795–803

D. Narendra, A. Tanaka, D.F. Suen, R.J. Youle. Parkin-induced mitophagy in the pathogenesis of Parkinson disease. Autophagy, 5 (2009), pp. 706–708

M.D. Neely, M.J. Litt, A.M. Tidball, G.G. Li, A.A. Aboud, C.R. Hopkins et al. DMH1, a highly selective small molecule BMP inhibitor promotes neurogenesis of hiPSCs: comparison of PAX6 and SOX1 expression during neural induction. ACS Chem Neurosci, 3 (6) (2012), pp. 482–491

K. Okita, Y. Matsumura, Y. Sato, A. Okada, A. Morizane, S. Okamoto et al. A more efficient method to generate integration-free human iPS cells. Nat Meth (2011), pp. 409–412

C.W. Olanow. Manganese-induced Parkinsonism and Parkinson's disease. Ann NY Acad Sci, 1012 (2004), pp. 209–223

P. Piccini, D.J. Burn, R. Ceravolo, D. Maraganore, D.J. Brooks. The role of inheritance in sporadic Parkinson's disease: evidence from a longitudinal study of dopaminergic function in twins. Ann Neurol, 45 (1999), pp. 577–582

J.R. Prohaska. Functions of trace elements in brain metabolism. Physiol Rev, 67 (1987), pp. 858–901

B.A. Racette, M. Aschner, T.R. Guilarte, U. Dydak, S.R. Criswell, W. Zheng. Pathophysiology of manganese-associated neurotoxicity. Neurotoxicology, 33 (4) (2011), pp. 881–886

J.A. Roth. Homeostatic and toxic mechanisms regulating manganese uptake, retention, and elimination. Biol Res, 39 (2006), pp. 45–57

J.A. Roth, L. Feng, J. Walowitz, R.W. Browne. Manganese-induced rat pheochromocytoma (PC12) cell death is independent of caspase activation. J Neurosci Res, 61 (2000), pp. 162–171

J.A. Roth, B. Ganapathy, A.J. Ghio. Manganese-induced toxicity in normal and human B lymphocyte cell lines containing a homozygous mutation in parkin. Toxicol In Vitro, 26 (2012), pp. 1143–1149

J.A. Roth, S. Singleton, J. Feng, M. Garrick, P.N. Paradkar. Parkin regulates metal transport via proteasomal degradation of the 1B isoforms of divalent metal transporter 1. J Neurochem, 113 (2010), pp. 454–464

A.H. Schapira. Aetiopathogenesis of Parkinson's disease. J Neurol, 258 (2011), pp. S307–S310

F.H. Sterky, S. Lee, R. Wibom, L. Olson, N.G. Larsson. Impaired mitochondrial transport and Parkin-independent degeneration of respiratory chain-deficient dopamine neurons in vivo. Proc Natl Acad Sci USA, 108 (2011), pp. 12937–12942

K. Takahashi, K. Tanabe, M. Ohnuki, M. Narita, T. Ichisaka, K. Tomoda et al. Induction of pluripotent stem cells from adult human fibroblasts by defined factors. Cell, 131 (2007), pp. 861–872

C. Tamm, F. Sabri, S. Ceccatelli. Mitochondrial-mediated apoptosis in neural stem cells exposed to manganese. Toxicol Sci, 101 (2008), pp. 310–320

C.M. Tanner, F. Kamel, G.W. Ross, J.A. Hoppin, S.M. Goldman, M. Korell et al. Rotenone, paraquat, and Parkinson's disease. Environ Health Perspect, 119 (2011), pp. 866–872

J.M. Vance, S. Ali, W.G. Bradley, C. Singer, D.A. Di Monte. Gene–environment interactions in Parkinson's disease and other forms of parkinsonism. Neurotoxicology, 31 (2010), pp. 598–602

R. von Coelln, V.L. Dawson, T.M. Dawson. Parkin-associated Parkinson's disease. Cell Tissue Res, 318 (2004), pp. 175–184

J. Wang, M.F. Rahman, H.M. Duhart, G.D. Newport, T.A. Patterson, R.C. Murdock et al. Expression changes of dopaminergic system-related genes in PC12 cells induced by manganese, silver, or copper nanoparticles. Neurotoxicology, 30 (2009), pp. 926–933

B.B. Williams, D. Li, M. Wegrzynowicz, B.K. Vadodaria, J.G. Anderson, G.F. Kwakye et al. Disease-toxicant screen reveals a neuroprotective interaction between Huntington's disease and manganese exposure. J Neurochem, 112 (2010), pp. 227–237

Z. Yin, J.L. Aschner, A.P. dos Santos, M. Aschner. Mitochondrial-dependent manganese neurotoxicity in rat primary astrocyte cultures. Brain Res, 1203 (2008), pp. 1–11

Z. Yin, H. Jiang, E.S. Lee, M. Ni, K.M. Erikson, D. Milatovic et al. Ferroportin is a manganese-responsive protein that decreases manganese cytotoxicity and accumulation. J Neurochem, 112 (2010), pp. 1190–1198

F. Zhang, Z. Xu, J. Gao, B. Xu, Y. Deng. In vitro effect of manganese chloride exposure on energy metabolism and oxidative damage of mitochondria isolated from rat brain. Environ Toxicol Pharmacol, 26 (2008), pp. 232–236

S. Zhang, J. Fu, Z. Zhou. In vitro effect of manganese chloride exposure on reactive oxygen species generation and respiratory chain complexes activities of mitochondria isolated from rat brain. Toxicol In Vitro, 18 (2004), pp. 71–77

X. Zhang, C.T. Huang, J. Chen, M.T. Pankratz, J. Xi, J. Li et al. Pax6 is a human neuroectoderm cell fate determinant. Cell Stem Cell, 7 (2010), pp. 90–100